AD-A270 532

ON PAGE

Form Approved
OMB No. 0704-0188

1. A	June 1993	3. REPORT TYPE AND DATES COVERED

4. TITLE AND SUBTITLE
Approximate evaluation of the spectral density integral for a large planar array of rectangular sensors excited by turbulent flow

5. FUNDING NUMBERS
PE - 63504
TA - S0223
WU - DN780-137

6. AUTHOR(S)
William Thompson, Jr. and Robert E. Montgomery

7. PERFORMING ORGANIZATION NAME(S) AND ADDRESS(ES)
NAVAL RESEARCH LABORATORY
UNDERWATER SOUND REFERENCE DETACHMENT
PO BOX 568337
ORLANDO FL 32856-8337

8. PERFORMING ORGANIZATION REPORT NUMBER

9. SPONSORING/MONITORING AGENCY NAME(S) AND ADDRESS(ES)

10. SPONSORING/MONITORING AGENCY REPORT NUMBER

11. SUPPLEMENTARY NOTES

12a. DISTRIBUTION/AVAILABILITY STATEMENT
Approved for public release; distribution unlimited.

12b. DISTRIBUTION CODE

13. ABSTRACT *(Maximum 200 words)*

An approximate numerical procedure has been developed for rapidly evaluating the spectral density integral that predicts the output of a planar array of many sensors excited by turbulent boundary layer pressure fluctuations. This procedure is particularly useful in cases where the transfer function factor of the integrand is not a simple function of the wave numbers in the flow and transverse directions. The procedure exploits the facts that the entire integrand is a seperable function of these two wave numbers and, when the number of sensors is large, the array function factor of the integrand is a rapidly varying function of wave number, characterized by many similar shaped lobes. In addition, a model for multilayered media is employed to provide the transfer function for boundary conditions that closely correspond to reality. Results generated by this procedure were compared to those from an exact evaluation of the integral which is possible if the transfer function is taken to be constant; there was agreement to within 0.2dB or better over a broad frequency interval. Some results for a realistic transfer the sensors embedded at an arbitrary position within the layer.

14. SUBJECT TERMS		15. NUMBER OF PAGES
s Sonar Arrays Spectral Density Transfer Function	Turbulent Flow Wavenumber Spectrum	7 16. PRICE CODE

17. SECURITY CLASSIFICATION OF REPORT	18. SECURITY CLASSIFICATION OF THIS PAGE	19. SECURITY CLASSIFICATION OF ABSTRACT	20. LIMITATION OF ABSTRACT
UNCLASSIFIED	UNCLASSIFIED	UNCLASSIFIED	UL

GENERAL INSTRUCTIONS FOR COMPLETING SF 298

The Report Documentation Page (RDP) is used in announcing and cataloging reports. It is important that this information be consistent with the rest of the report, particularly the cover and title page. Instructions for filling in each block of the form follow. It is important to *stay within the lines* to meet *optical scanning requirements*.

Block 1. Agency Use Only *(Leave blank)*.

Block 2. Report Date. Full publication date including day, month, and year, if available (e.g. 1 Jan 88). Must cite at least the year.

Block 3. Type of Report and Dates Covered. State whether report is interim, final, etc. If applicable, enter inclusive report dates (e.g. 10 Jun 87 - 30 Jun 88).

Block 4. Title and Subtitle. A title is taken from the part of the report that provides the most meaningful and complete information. When a report is prepared in more than one volume, repeat the primary title, add volume number, and include subtitle for the specific volume. On classified documents enter the title classification in parentheses.

Block 5. Funding Numbers. To include contract and grant numbers; may include program element number(s), project number(s), task number(s), and work unit number(s). Use the following labels:

C	- Contract	PR	- Project
G	- Grant	TA	- Task
PE	- Program Element	WU	- Work Unit Accession No.

Block 6. Author(s). Name(s) of person(s) responsible for writing the report, performing the research, or credited with the content of the report. If editor or compiler, this should follow the name(s).

Block 7. Performing Organization Name(s) and Address(es). Self-explanatory.

Block 8. Performing Organization Report Number. Enter the unique alphanumeric report number(s) assigned by the organization performing the report.

Block 9. Sponsoring/Monitoring Agency Name(s) and Address(es). Self-explanatory.

Block 10. Sponsoring/Monitoring Agency Report Number. *(If known)*

Block 11. Supplementary Notes. Enter information not included elsewhere such as: Prepared in cooperation with...; Trans. of...; To be published in.... When a report is revised, include a statement whether the new report supersedes or supplements the older report.

Block 12a. Distribution/Availability Statement. Denotes public availability or limitations. Cite any availability to the public. Enter additional limitations or special markings in all capitals (e.g. NOFORN, REL, ITAR).

- DOD - See DoDD 5230.24, "Distribution Statements on Technical Documents."
- DOE - See authorities.
- NASA - See Handbook NHB 2200.2.
- NTIS - Leave blank.

Block 12b. Distribution Code.

- DOD - Leave blank.
- DOE - Enter DOE distribution categories from the Standard Distribution for Unclassified Scientific and Technical Reports.
- NASA - Leave blank.
- NTIS - Leave blank.

Block 13. Abstract. Include a brief *(Maximum 200 words)* factual summary of the most significant information contained in the report.

Block 14. Subject Terms. Keywords or phrases identifying major subjects in the report.

Block 15. Number of Pages. Enter the total number of pages.

Block 16. Price Code. Enter appropriate price code *(NTIS only)*.

Blocks 17. - 19. Security Classifications. Self-explanatory. Enter U.S. Security Classification in accordance with U.S. Security Regulations (i.e., UNCLASSIFIED). If form contains classified information, stamp classification on the top and bottom of the page.

Block 20. Limitation of Abstract. This block must be completed to assign a limitation to the abstract. Enter either UL (unlimited) or SAR (same as report). An entry in this block is necessary if the abstract is to be limited. If blank, the abstract is assumed to be unlimited.

Approximate evaluation of the spectral density integral for a large planar array of rectangular sensors excited by turbulent flow[a)]

William Thompson, Jr.
Department of Engineering Science and Mechanics and The Applied Research Laboratory, The Pennsylvania State University, University Park, Pennsylvania 16802

Robert E. Montgomery
Naval Research Laboratory, Underwater Sound Reference Detachment, P. O. Box 568337, Orlando, Florida 32856-8337

(Received 24 June 1992; revised 29 January 1993; accepted 16 February 1993)

An approximate numerical procedure has been developed for rapidly evaluating the spectral density integral that predicts the output of a planar array of many sensors excited by turbulent boundary layer pressure fluctuations. This procedure is particularly useful in cases where the transfer function factor of the integrand is not a simple function of the wave numbers in the flow and transverse directions. The procedure exploits the facts that the entire integrand is a separable function of these two wave numbers and, when the number of sensors is large, the array function factor of the integrand is a rapidly varying function of wave number, characterized by many similar shaped lobes. In addition, a model for multilayered media is employed to provide the transfer function for boundary conditions that closely correspond to reality. Results generated by this procedure were compared to those from an exact evaluation of the integral which is possible if the transfer function is taken to be constant; there was agreement to within 0.2 dB or better over a broad frequency interval. Some results for a realistic transfer function are presented, such as the case of an elastomeric layer backed by an elastic plate with the sensors embedded at an arbitrary position within the layer.

PACS numbers: 43.30.Yj, 43.30.Lz

INTRODUCTION

In a recent article, Ko and Nuttall[1] discuss the evaluation of the spectral density integral that predicts the response of a planar array of identical sensors when excited by boundary layer pressure fluctuations associated with turbulent fluid flow over the array. It is assumed that the turbulent field is spatially homogeneous and temporally stationary. This integral, denoted $Q(\omega)$ where ω is the radian frequency, has the form

$$Q(\omega)=2\pi\int_{-\infty}^{\infty}\int_{-\infty}^{\infty}A(k_x,k_y)S(k_x,k_y)T(k_x,k_y;\omega)\times P(k_x,k_y;\omega)dk_x\,dk_y, \quad (1)$$

where $P(k_x,k_y;\omega)$ is the turbulent boundary layer pressure spectrum. The transfer function $T(k_x,k_y;\omega)$ describes the wave-number filtering action of a layer of material, typically an elastomeric material, applied over the sensors to offset the turbulent boundary layer from the sensors. The transfer function expresses the magnitude of the ratio of the pressure at any point within that layer of material to the stress imposed by the pressure of the turbulent boundary layer acting on the "wet" face of the layer. The hydrophone function $S(k_x,k_y)$ is a measure of the spatial averaging associated with the size of each sensor. The array function $A(k_x,k_y)$ is also a measure of the spatial averaging effect associated with more than one sensor in both the x and y directions. Finally, k_x and k_y are the wave numbers in the x and y directions, respectively. The array of sensors lies in the x, y plane and the turbulent flow is assumed to be in the x direction. It should be noted that the expression for $Q(\omega)$ in Eq. (1) appears to differ by a factor of 2π from that given in a previous article by Ko and Schloemer.[2] There is, in fact, no numerical discrepancy between these two expressions because the factor of 2π has been incorporated into the integrand in the expression stated in Ref. 2.

It is necessary to examine the functional form of the factors of the integrand in Eq. (1) to both appreciate the problem at hand and to set the stage for the method that is espoused to evaluate the integral. Consider first the turbulent boundary layer pressure spectrum, $P(k_x,k_y;\omega)$. Various analytic descriptions of this spectrum have been proposed. A classic one, and that which was used by Ko and Nuttall,[1] is due to Corcos.[3] Recently, Ko[4] also considered a modification that predicts a much lower spectrum level at very small wave numbers than the original Corcos model. Because of the desire to compare results with those of Ref. 1, only the original Corcos model is considered here:

$$P(k_x,k_y;\omega)=\frac{P(0,\omega)(\alpha_1\alpha_2 k_c^2)}{\pi^2[(k_x-k_c)^2+(\alpha_1 k_c)^2][k_y^2+(\alpha_2 k_c)^2]}, \quad (2)$$

where $k_c=\omega/u_c$ is the convective wave number and u_c is the convective flow speed that is taken to be 60% of the free-stream velocity U. The flow is assumed to be only in

[a)]Portions of this paper were presented at the 120th meeting of the Acoustical Society of America [J. Acoust. Soc. Am. Suppl. 1 **88**, S6 (1990)].

 0001-4966/93/063201-07$06.00

the x direction. The quantities α_1 and α_2 are dimensionless constants that are chosen to effect a good match of Eq. (2) with data. The set of values used in Ref. 1 is $\alpha_1=0.09$ and $\alpha_2=0.63$. The quantity $P(0,\omega)$ is called the point power spectrum and is described by

$$P(0,\omega)=\alpha_3\rho_0^2 v_*^4/\omega, \tag{3}$$

where ρ_0 is the density of the fluid medium; v_* is the friction, or shear velocity, which is taken to be 3.5% of the free-stream velocity; and α_3 is another dimensionless constant for which an appropriate value[1] is 1.064. An important feature of the Corcos spectrum as described by Eq. (2) is that it is a separable function of the two wave numbers k_x and k_y, i.e., it can be written as the product of a function of k_x times a function of k_y.

For a rectangular-shaped sensor of dimensions L_x and L_y, whose edges are, respectively, oriented along the flow and transverse directions, the hydrophone function is[5,6]

$$S(k_x,k_y)=\left(\frac{\sin(k_xL_x/2)}{k_xL_x/2}\,\frac{\sin(k_yL_y/2)}{k_yL_y/2}\right)^2. \tag{4}$$

This expression is simply the square of the magnitude of the normalized directivity function associated with the size and shape of the sensor, expressed as a function of the variable wave numbers k_x and k_y rather than as a function of the frequency, where the signal—the turbulent pressure wave—impinges upon the sensor at grazing incidence. For this shape and orientation of the sensor, $S(k_x,k_y)$ is also a separable function of k_x and k_y. This feature would not exist for some other shapes such as circular sensors.

For a rectangular array of equally spaced, in phase, identical sensors, the array function is[7]

$$A(k_x,k_y)=\left(\frac{\sin(N_xk_xd_x/2)}{N_x\sin(k_xd_x/2)}\,\frac{\sin(N_yk_yd_y/2)}{N_y\sin(k_yd_y/2)}\right)^2, \tag{5}$$

where N_x and N_y are the numbers of sensors along the x and y directions, respectively, and d_x and d_y are the center-to-center spacings, respectively (Fig. 1). When N_x or N_y is large, the array function, and hence the integrand in Eq. (1), are rapidly varying functions of wave number. In such cases conventional quadrature techniques for performing the integrations in Eq. (1) can be inefficient or impractical. This paper presents an alternative technique that is both fast and accurate for cases where conventional quadrature techniques become impractical. The method is not applicable to small arrays (N_x or $N_y<5$), however there is no need in such cases because conventional methods may be easily implemented. The array function is the square of the magnitude of the normalized directivity function of an array of point sensors with the same relative amplitudes, phases, and center-to-center spacings as those of the actual sensors, expressed as a function of variable wave numbers k_x and k_y, again for the case of grazing incidence excitation. The product of the two functions $A(k_x,k_y)$ and $S(k_x,k_y)$ is a statement of the classic product theorem for the response function of an array of transducers of identical size, shape, and orientation. In the case where beam steering has been implemented to direct the maximum

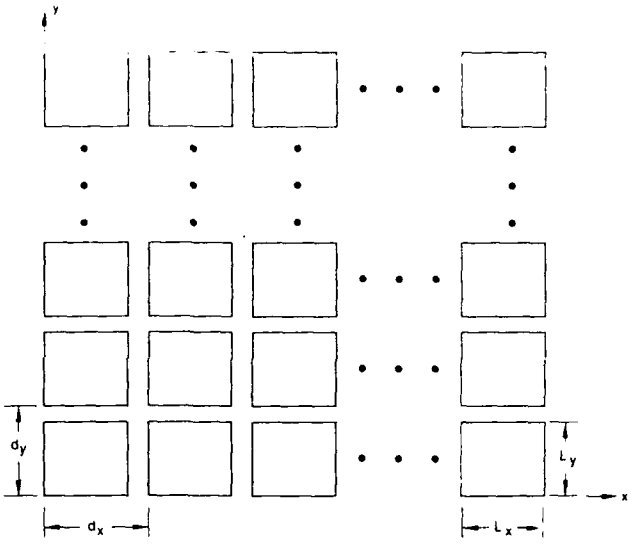

FIG. 1. Planar grid of rectangular sensors, N_x along x axis by N_y along y axis.

acoustic response of the array to some direction other than broadside, the arguments k_x and k_y in the array function will accordingly be translated in wave number space by appropriate amounts k_{Sx} and k_{Sy} so that the array function takes the form:

$$A(k_x,k_y)=\left(\frac{\sin[N_x(k_x-k_{Sx})d_x/2]}{N_x\sin[(k_x-k_{Sx})d_x/2]}\,\frac{\sin[N_y(k_y-k_{Sy})d_y/2]}{N_y\sin[(k_y-k_{Sy})d_y/2]}\right)^2. \tag{6}$$

It is noted that the array function is also a separable function of k_x and k_y.

I. STATEMENT OF THE PROBLEM

For the special case where $T=1.0$, i.e., there is no elastomeric layer over the array of sensors, the integral in Eq. (1) can be evaluated exactly. Ko and Nuttall[1] do this both by residue calculus and by a clever application of Parseval's theorem. Since all three remaining factors in the integrand of Eq. (1) are separable functions of k_x and k_y, the double integral simplifies to the product of two similar integrals, one over the domain of k_x and the other over k_y.

For the case of a realistic overlayer between the sensors and the turbulent flow, however, the transfer function T becomes complicated. Ko and Schloemer[2] discuss the case of a single homogeneous elastomer layer with a rigid backing and with the sensors embedded at an arbitrary position within the layer. In this case, evaluating T involves solving a fourth-order system of linear algebraic equations whose coefficients are not simple. For a more realistic condition, such as the elastomer layer on an elastic base plate, T is even more complicated.

An analytical method exists that permits rapid numerical evaluation of the transfer function for a harmonic plane wave incident upon a laterally infinite medium that contains any number of material layers bounded on either

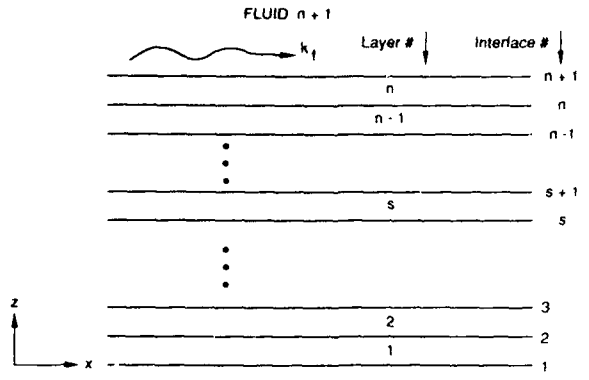

FIG. 2. Transverse cross section of multilayered model used to obtain the transfer function. Layers are laterally infinite and may contain solid or fluid material. The sensor is located at interface s.

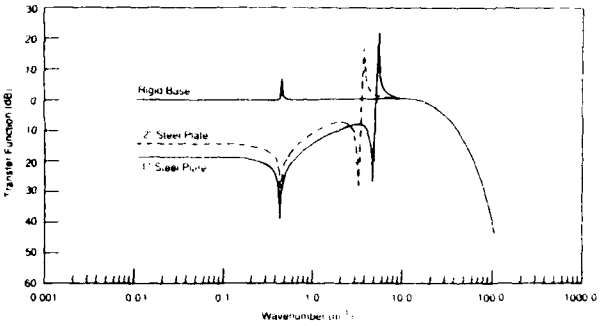

FIG. 3. Transfer function at 100 Hz for a 0.0762-m (3-in.)-thick elastometer layer (material properties as described in text) for three different base structures as a function of wave number. The sensors are located 0.00635 m (0.25 in.) above the base.

side by fluids extending to infinity as illustrated by Fig. 2. This method, originally expounded by Brekhovskikh,[8] is based upon matching velocity and pressure variables at each boundary of the layered medium. This leads to an analytical matrix expression as follows:

$$\begin{bmatrix} v_x^{(i+1)} \\ v_z^{(i+1)} \\ \tau_{zz}^{(i+1)} \\ \tau_{zx}^{(i+1)} \end{bmatrix} = \mathbf{A}^{(i)} \begin{bmatrix} v_x^{(i)} \\ v_z^{(i)} \\ \tau_{zz}^{(i)} \\ \tau_{zx}^{(i)} \end{bmatrix}, \tag{7}$$

where $\mathbf{A}^{(i)}$ is a 4×4 matrix that relates velocities v_x, v_z and stresses τ_{zz}, τ_{zx} at interface i to the corresponding velocities and stresses at interface $i+1$. Analytical expressions for the components of $\mathbf{A}^{(i)}$ are conveniently tabulated in Ref. 9. For the purpose of computing a transfer function, one needs a relationship that expresses the normal stress $\tau_{zz}^{(s)}$ at the sensor in terms of the normal stress, $\tau_{zz}^{(n+1)}$, at interface $n+1$ where the acoustic plane wave of amplitude p_0 is assumed to be incident. This can be accomplished by applying Eq. (7), in turn, to each of the intervening layers that separate the sensor from the interface where the excitation is incident. In this way, the dynamic variables at any interface are related to the corresponding dynamic variables at any other interface by a matrix that is the product of the $\mathbf{A}^{(i)}$ matrices for the intervening layers, the order of this product being the same as the order of the intervening layers. Referring to Fig. 2, the transfer function can be expressed as

$$T = \left| \frac{\tau_{zz}^{(s)}}{\tau_{zz}^{(n+1)}} \right|^2. \tag{8}$$

By imposing the appropriate boundary conditions at interfaces 1 and $n+1$, one obtains a set of equations from which T can be evaluated. Note that $\tau_{zx}^{(1)} = \tau_{zx}^{(n+1)} = 0$ because the fluids do not support shear stress. Also, the normal stress at a fluid interface can be related to the normal velocity; for example,[10] at interface $n+1$

$$\tau_{zz}^{(n+1)} = p_0 - j\rho_0\omega v_z^{(n+1)} / \sqrt{k^2 - k_f^2}, \tag{9}$$

where k is the acoustic wave number in the fluid and k_f is the wave number of the imposed wave component. The term containing $v_z^{(n+1)}$ accounts for the pressure radiated at $n+1$, whereas p_0 represents a spectral component of flow noise. In this paper it is assumed that fluid 1 is a vacuum and therefore $\tau_{zz}^{(1)} = 0$. Now, using the multilayered matrix model described above, one can write

$$\tau_{zz}^{(s)} = P_{31} v_x^{(n+1)} + P_{32} v_z^{(n+1)} + P_{33} \tau_{zz}^{(n+1)}, \tag{10a}$$

$$\tau_{zx}^{(1)} = 0 = Q_{41} v_x^{(n+1)} + Q_{42} v_z^{(n+1)} + Q_{43} \tau_{zz}^{(n+1)}, \tag{10b}$$

and

$$\tau_{zz}^{(1)} = 0 = Q_{31} v_x^{(n+1)} + Q_{32} v_z^{(n+1)} + Q_{33} \tau_{zz}^{(n+1)}, \tag{10c}$$

where the components of the $\mathbf{P}$ and $\mathbf{Q}$ matrices are found by taking the products of the $\mathbf{A}^{(i)}$ matrices of the intervening layers. The transfer function can now be obtained from Eq. (10a), with $\tau_{zz}^{(n+1)}$ eliminated by using Eq. (9), and with $v_x^{(n+1)}$ and $v_z^{(n+1)}$ eliminated using Eqs. (10b) and (10c). The resulting expression is analytic but too complex to permit an analytic evaluation of $Q(\omega)$. However, numerical evaluation of T at discrete values of the wave numbers is quite easy.

Figure 3 illustrates the transfer function (decibel scale) as a function of wave number at a frequency of 100 Hz for the case of a 0.0762-m (3-in.) elastomer layer on different base structures; i.e., a perfectly rigid base or two different thicknesses of a vacuum-backed steel plate. The parameters of the elastomer material are chosen as follows: shear speed, 16.7 m/s; dilatational speed, 2000 m/s; shear loss factor, 0.33; dilatational loss factor, 0.03; density 1200 kg/m^3. These parameter values do not represent a realistic material. They were simply chosen to correspond to the values used in Ref. 2. The point within the layer where the transmitted pressure is monitored is taken to be 0.00635 m (0.25 in.) above the bottom face of the elastomer layer. Observe that the two curves for bases plates of finite thickness are significantly different from the curve for the rigid base at low wave numbers. The low wave-number spike seen in all three curves occurs at the acoustic wave number. The subsequent large excursions on the two different steel plate curves occur at their respective flexural wave

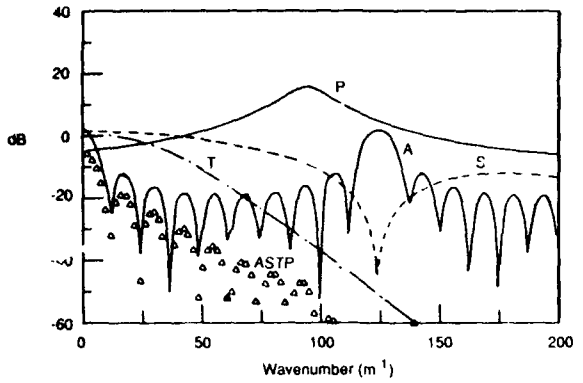

FIG. 4. The four factors of the integrand of the $Q(\omega)$ integral plotted as a function of wave number at a frequency of 100 Hz for a 10 by 10 array of 0.0508-m (2-in.)-square contiguous sensors. All other parameters as described in the text. The transfer function curve is the rigid base curve from Fig. 3. The reference value for the P curve and the ASTP curve is 1.0 (Pa-m^2/Hz).

numbers. All the curves coalesce for large wave numbers, showing a rolloff that occurs around the shear wave number in the elastomer layer. There is a significant difference at low wave numbers between the curves for the rigid boundary condition and the elastic plate base boundary condition, and this will subsequently be seen to have a significant effect upon the value of $Q(\omega)$.

Suffice it to say that in the absence of a simple analytic expression for T, the integral in Eq. (1) cannot be evaluated to obtain a closed form expression for $Q(\omega)$. Furthermore, standard numerical quadrature routines have been found to require copious amounts of CPU time. This article discusses an approximate numerical procedure for evaluating the integral in this circumstance that has been found to be both fast and quite accurate.

II. ANALYSIS

Figure 4 is a plot of each of the four factors that comprise the integrand of Eq. (1) and their product as a function of wave number k_x in the flow direction for the fixed value of $k_y=0$ and for the following choice of parameters: $U=10.288$ m/s (20 kn.), $N_x=N_y=10$, $L_x=L_y=d_x=d_y=0.0508$ m (2 in.), $k_{Sx}=k_{Sy}=0$, frequency $=100$ Hz, and the transfer function is the curve for a rigid base boundary condition in Fig. 3. A similar plot vs k_y would be obtained for a fixed k_x, except there is no peak in the pressure spectrum for any wave number in the direction transverse to the flow. Because of the product nature of the integrand, Eq. (1) reduces to the product of two similar integrals, one over the domain of k_x, and the other over k_y. It is evident that the controlling factor among the four is the array function $A(k_x,k_y)$ in the sense that it is the most rapidly varying function of the integration variable k_x (or k_y); i.e., over the range of k_x or k_y that defines one lobe of the array function, the other three factors S, T, and P do not vary greatly and can be considered to be essentially constant. This feature becomes more pronounced with increasing N_x or N_y as more and more sidelobes are present between adjacent grating lobes of the A function. Furthermore, the shape of every one of the sidelobes of the array function appears to be the same (note that the discretization used in generating this plot has blurred the fact that there are true zeros of the array function). Consequently, if the integral over any one sidelobe of just the array function, when renormalized to a maximum height of unity, was found to be a constant, i.e., independent of wave number, then the integral of the product ASTP over that sidelobe could be approximated as that constant times the values of the A, S, T, and P functions evaluated at the wave number corresponding to the peak of that sidelobe. Integration over all sidelobes would then entail a simple summation.

Consider the integral of one sidelobe of the normalized array function; call this quantity I_x. To normalize a sidelobe to unit height, note that the factor $\sin(k_xd_x/2)$ in the denominator is not a rapidly varying function of k_x over the interval of that sidelobe. Hence, the quantity $N_x \sin(k_xd_x/2)$ is equated to unity, and the integral in question can be written

$$I_x \approx \frac{2}{d_x}\int_{\pi/N_x}^{2\pi/N_x} [\sin(N_x\zeta)]^2\, d\zeta = \frac{\pi}{N_xd_x}, \tag{11}$$

where $\zeta=k_xd_x/2$. The indicated limits define the first sidelobe; however, the result is found to be the same for any other normalized sidelobe. The integral in the k_y direction over any one sidelobe is formally the same result except for an obvious change in subscripts.

The mainlobe and all grating lobes of the A function are of different shape than the sidelobes, and these lobes extend over a range of wave numbers that is twice as large as that which defines a sidelobe. The integral over half of the mainlobe or any grating lobe, denoted I_0, takes the form

$$I_0=\frac{2}{d_x}\int_0^{\pi/N_x}\left[\frac{\sin N_x\zeta}{N_x\sin\zeta}\right]^2 d\zeta. \tag{12}$$

This integrand is already normalized to a maximum value of unity. To evaluate this it is convenient to note that

$$\frac{\sin N_x\zeta}{N_x\sin\zeta}=\frac{2}{N_x}\left(0.5+\sum_{i=1}^{(N_x-1)/2}\cos(2i\zeta)\right),$$

$$\text{for } N_x \text{ odd and } >1 \tag{13a}$$

$$=\frac{2}{N_x}\sum_{i=1}^{N_x/2}\cos(2i-1)\zeta, \quad \text{for } N_x \text{ even and } \geqslant 2. \tag{13b}$$

Hence,

$$I_0=\frac{2}{N_x^2d_x}\left[\frac{\pi}{N_x}+2\sum_{i=1}^{(N_x-1)/2}\frac{1}{i}\sin\left(\frac{2\pi i}{N_x}\right)\right.$$

$$\left.+\sum_{i=1}^{(N_x-1)/2}\sum_{j=1}^{(N_x-1)/2}\left(\frac{\sin[(i-j)2\pi/N_x]}{(i-j)}+\frac{\sin[(i+j)2\pi/N_x]}{(i+j)}\right)\right], \quad \text{for } N_x \text{ odd and } >1 \tag{14a}$$

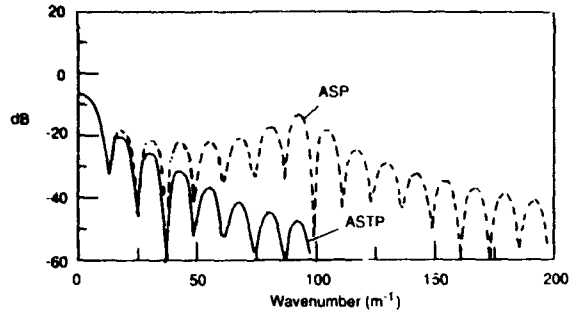

FIG. 5. Comparison of the integrand of Eq. (1) for the cases $T=1.0$ and T as in Fig. 4. All other parameters as in Fig. 4.

$$=\frac{2}{N_x^2 d_x}\sum_{i=1}^{N_x/2}\sum_{j=1}^{N_x/2}\left(\frac{\sin[(i+j-1)2\pi/N_x]}{(i+j-1)}+\frac{\sin[(i-j)2\pi/N_x]}{(i-j)}\right),\quad \text{for } N_x \text{ even and } \geqslant 2. \tag{14b}$$

This result for the integral over one-half of either the mainlobe or any grating lobe was compared with the result in Eq. (11) for the integral over any normalized sidelobe. The result in Eq. (14) is somewhat smaller and for large N_x approaches a value which is approximately 90% of Eq. (11). In the computational procedure described below, the exact value of I_0 as computed from Eq. (14) is used.

The integral in Eq. (1) is then approximated as follows. Reiterating that the integrand is a separable function of k_x and k_y, and that the integrals over the k_x and k_y variables are similar in form, consider, therefore, only the k_x integral

$$Q_x(\omega)=\int_{-\infty}^{\infty} A(k_x)S(k_x)T(k_x;\omega)P(k_x;\omega)dk_x. \tag{15}$$

First, large finite values are chosen for the upper and lower limits based upon knowledge of how the integrand decreases with increasing $|k_x|$. The controlling factor in this regard is usually $T(k_x;\omega)$. Figure 5 shows the integrand for two different values of T; the solid line curve repeats the ASTP curve from Fig. 4, while the dashed line curve is the case $T=1.0$. Since the transfer function is an even function of k_x, limits of ± 150 m^{-1} would appear to be sufficient for integration of the former curve, while the limits should be increased to about ± 300 m^{-1} for the latter. Since the integrand is positive, a lower bound on the exact value will be realized by restricting the limits. Assuming the functions S, T, and P to be essentially constant over the interval of either one sidelobe or one-half of either the mainlobe or a grating lobe, $Q_x(\omega)$ is then approximated as

$$Q_x(\omega)=\sum_i S(k_{x,i})T(k_{x,i};\omega)P(k_{x,i};\omega)\int_{\text{lobe}_i} A(k_x)dk_x, \tag{16}$$

where the indicated summation extends over all the lobes within the chosen limits of integration. The values $k_{x,i}$ denote the maxima of the A function in the interval of integration and are determined by finding the roots of the transcendental equation that results from setting the derivative of the A function with respect to k_x equal to zero:

$$N_x \sin\left(\frac{k_x d_x}{2}\right)\cos\left(\frac{N_x k_x d_x}{2}\right)-\sin\left(\frac{N_x k_x d_x}{2}\right)\cos\left(\frac{k_x d_x}{2}\right)=0. \tag{17}$$

The remaining integral in Eq. (16) is then either approximated as $\pi/N_x d_x$ times the value of the array function at $k_{x,i}$ for any sidelobe, or the value predicted by Eq. (14) for either half of the mainlobe or any grating lobe. Hence,

$$Q_x(\omega)\approx\frac{\pi}{N_x d_x}\sum_i \alpha_i A(k_{x,i})S(k_{x,i})T(k_{x,i};\omega)P(k_{x,i};\omega), \tag{18}$$

where $\alpha_i=1$ if i denotes a sidelobe, but $\alpha_i=N_x d_x I_0/\pi$ if i denotes either half of the mainlobe, or either half of any grating lobe; again, the latter values of α_i vary with N_x and are numbers slightly greater than 0.9.

Since the integral over k_y is formally the same, the final result for $Q(\omega)$ is

$$Q(\omega)=\frac{2\pi^3}{N_x N_y d_x d_y}\left(\sum_i \alpha_i A(k_{x,i})S(k_{x,i})T(k_{x,i};\omega)P(k_{x,i};\omega)\right)\times\left(\sum_j \alpha_j A(k_{y,i})S(k_{y,i})T(k_{y,j};\omega)P(k_{y,j};\omega)\right). \tag{19}$$

III. RESULTS AND DISCUSSION

A FORTRAN language computer program was developed to generate numerical results from Eq. (19). An IMSL routine was used to find the roots of Eq. (17), i.e., the $k_{x,i}$ values, in the interval between the peak of the mainlobe and the peak of the first grating lobe. The remainder of the $k_{x,i}$ values within the chosen limits of integration are obtained simply by noting the periodic nature of the array function. These values, shifted by k_{Sx} if appropriate, are then stored. The same procedure produces the set $k_{y,j}$. Note that under this counting system the entire mainlobe and every grating lobe is accounted for by two successive values of index i or j with identical values of $k_{x,i}$ or $k_{y,j}$. The indicated summations in Eq. (19) are then performed in straightforward fashion to produce $Q(\omega)$.

The analysis and computer program were checked by calculating $Q(\omega)$ for the set of parameter values used by Ko and Nuttall,[1] viz., a 10 by 10 array of contiguous 0.0508-m (2-in.)-square sensors with no elastomer overlayer ($T=1.0$), a free-stream velocity of 10.288 m/s and a frequency range of 100 Hz to 2 kHz. The results obtained matched their exact values within 0.2 dB over the whole frequency range. In all cases the values obtained from the approximate expression are smaller than the exact values. The approximate expression should become more accurate as the frequency of the sidelobes of the array function A increases (i.e., as either parameter N_x and N_y increases)

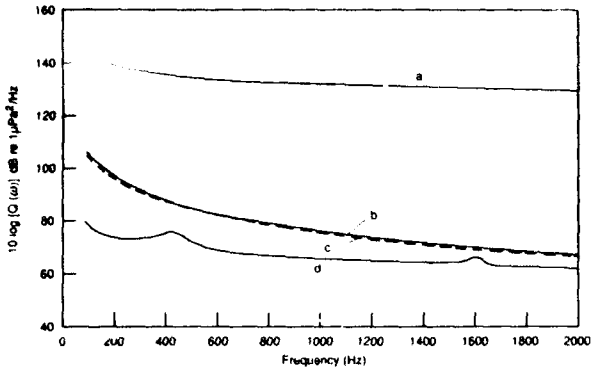

FIG. 6. Spectral density level for various situations: (a) one point sensor and unity transfer function; (b) a 10 by 10 array of contiguous 0.0508-m (2-in.)-square sensors and unity transfer function; (c) case (b) with a 0.0762-m (3-in.) overlayer of elastomer with a rigid base, sensors 0.00635 m (0.25 in.) above base; (d) same as (c) except base is a vacuum backed 0.0254-m (1-in.)-thick steel plate. All other parameters as defined in the text.

because the assumption that the S, T, and P functions are constant over a sidelobe of the A function then becomes more valid. That this is the case can be demonstrated by subdividing the array into a larger number of smaller contiguous sensors that cover the 20-in.-square surface. The exact result for $Q(\omega)$ should be the same. Hence, the approximate expression was used to calculate $Q(\omega)$ for a 20 by 20 array of 0.0254-m-square sensors and 40 by 40 array of 0.0127-m-square sensors. The computation time was not perceptibly increased in spite of the doubling and quadrupling of the number of terms to be summed. As expected, the accuracy of approximation improved. The $Q(\omega)$ values increased slightly to within 0.1 dB of the exact values.

To illustrate the effect of including a nonconstant transfer function in the computations, the results shown in Fig. 6 were generated. For wave number tilts k_{Sx} and k_{Sy} of zero, the spectral density level is plotted as a function of frequency for the cases of (a) one point sensor with no elastomer overlayer so that $T=1.0$; (b) a 10 by 10 array of contiguous 0.0508-m-square sensors, again with $T=1$ (these first two cases are data from Ref. 1); (c) case (b) with a 0.0762 m thick overlayer of elastomer (material properties defined earlier) with a rigid base where the sensors are 0.00635 m above the rigid base; (d) same as (c) except the rigid base is replaced by a vacuum backed 0.0254-m-thick steel plate. The transfer functions for cases (c) and (d) are plotted in Fig. 3 for a frequency of 100 Hz. There is evidently not much difference in $Q(\omega)$ for cases (b) and (c). As is apparent from Fig 3, the transfer function at 100 Hz for the rigid-backed-elastomer-layer situation is essentially unity up to a wave number of 20 m^{-1} which, noting the plots of the integrand in Fig. 5, is large enough to include most of the wave number region that contributes to $Q(\omega)$. Consequently, the integral is not much affected by the high wave number rolloff of T. Conversely, the smaller transfer function associated with the more realistic case of the vacuum backed steel base plate results in a noticeably lower value of $Q(\omega)$, particularly at the low end of the frequency range. The bumps in curve (d) at 440 and 1600 Hz are consequences of certain peaks in the transfer function, such as the one associated with the shear wavelength, becoming coincident with the peak of a high sidelobe of the array function. Note that in this special case of contiguous sensors, the nulls of the S function coincide with the peaks of the grating lobes of the A function, and hence there are no grating lobes. Were that not the case, there would probably also be a large bump in the $Q(\omega)$ curve at frequencies where the peak of the P curve coincided with a grating lobe.

IV. CONCLUSION

An approximate numerical technique has been developed for evaluating the spectral density integral over all wave numbers to obtain the output of a large planar array of sensors being excited by turbulent boundary layer pressure fluctuations. This technique is fast [for comparison, $Q(\omega)$ for the above case where $T=1.0$ was also evaluated using the IMSL numerical quadrature routine QDAGS and the elapsed CPU time was found to be almost twice as much as for this approximate technique] and is quite accurate as determined by comparing the results with those for cases where the integrals in question can be evaluated exactly. Most importantly, it can be used when it is not possible to evaluate the integrals exactly, such as when a simple analytic expression for the transfer function is not available. All that is required for this technique is knowledge of the value of the transfer function at a discrete set of wave number values. It has also been demonstrated how numerical values for the transfer function may be easily obtained for multilayered array models that more closely resemble reality than for models that assume rigid substrates. The technique for computing $Q(\omega)$ for exploits the fact that the array function is the most rapidly varying function of wave number of all the factors of the integrand, and assumes that the other factors may be considered to be constant over the wave number interval corresponding to one lobe of the array function. Consequently, the accuracy of the technique increases as the number of sensors increases, since that number is a measure of the number of lobes between adjacent grating lobes of the array function. The technique is restricted to situations where all the factors of the integrand are separable functions of the wave numbers in the flow direction and transverse to that direction. Hence a regular grid of circular shaped sensors, or an irregularly spaced array of rectangular sensors, could not be evaluated by this technique. The technique was illustrated for the case of contiguous sensors but is, in no way, limited to this case. Gaps of any size may be considered between sensors as long as the gap sizes are uniform along each lateral direction.

ACKNOWLEDGMENTS

This work was sponsored by The Naval Sea Systems Command. A portion of this work was performed by William Thompson, Jr. while on sabbatic leave at the Naval Research Laboratory.

[1]S. H. Ko and A. H. Nuttall, "Analytical evaluation of flush-mounted hydrophone array response to the Corcos turbulent wall pressure spectrum," J. Acoust. Soc. Am. **90**, 579–588 (1991).

[2]S. H. Ko and H. H. Schloemer, "Calculations of turbulent boundary layer pressure fluctuations transmitted into a viscoelastic layer," J. Acoust. Soc. Am. **85**, 1469–1477 (1989).

[3]G. M. Corcos, "The structure of the turbulent pressure field in boundary layer flows," J. Fluid Mech. **18**, 353–378 (1964).

[4]S. H. Ko, "Analytical evaluation of a flush-mounted hydrophone array response to a modified Corcos turbulent wall pressure spectrum," NUSC Tech Rep. 8943, Naval Underwater Systems Center (1991).

[5]P. H. White, "Effect of transducer size, shape, and surface sensitivity on the measurement of boundary-layer pressures," J. Acoust. Soc. Am **41**, 1358–1363 (1967).

[6]D. M. Chase, "Turbulent-boundary layer pressure fluctuations and wave number filtering by nonuniform spatial averaging," J Acoust. Soc. Am. **46**, 1350–1365 (1969).

[7]W. K. Blake, *Mechanic of Flow Induced Sound and Vibration* (Academic, Orlando, 1986), Vol. II, pp. 562–569.

[8]L. M. Brekhovskikh, *Waves in Layered Media* (Academic, Orlando, 1980), 2nd ed., Sec. 8.3.

[9]D. L. Folds and C. D. Loggins, "Transmission and reflection of ultrasonic waves in layered media," J. Acoust. Soc. Am. **62**, 1102–1109 (1977).

[10]M. C. Junger and D. Feit, *Sound, Structures and Their Interaction* (MIT, Cambridge, MA, 1986), 2nd ed., pp. 131–134.